Al-Qadisiyah Journal for Engineering Sciences 16 (2023) 127–132

Contents lists available at http://qu.edu.iq

Al-Qadisiyah Journal for Engineering Sciences

Journal homepage: http://qu.edu.iq/journaleng/index.php/JQES

Parameters estimation of non-saturated permanent magnet synchronous machines by aid of statistical analysis

Mazen M. A. Al Ibraheemi [a*], ***Fatih J. Anayi*** [b], ***Zainb H. Radhy*** [c] ***and Mahdi W. Neamah*** [c]

[a]*Department of Electronics and Communication, College of Engineering, University of Al Qadisiyah, Iraq*
[b]*Wolfson Centre for Magnetics, Cardiff University, Cardiff CF24 3AA, U.K*
[c]*Department of Statistics, College of Administration and Economics, Karbala University, Karbala, Iraq*

ARTICLE INFO

Article history:
Received 25 December 2022
Received in revised form 25 February 2023
Accepted 20 June 2023

Keywords:
Synchronous Machines
Rotor Position
Signals
Sensorless Technique
Voltage

ABSTRACT

The rotor position value is the most important parameter in synchronous machines. In this paper, a MATLAB model of high-resolution rotor position determination at zero speed, without any position sensor, is presented for a non-saturated permanent magnet motor. The motor current and voltage responses for two short pulses were employed to form address lines for memory cells whose contents represent the exact rotor position. The proposed model presents rotor position at 1^{o} resolution and works with salient rotor poles. It could be modified to obtain the results for non-salient poles. The model needs only two current sensors and does not require any special technique for magnet polarity detection. This method was tested successfully for a two-poles machine, and it could be applicable to any number of poles. The statistical analysis, regarding the uniform distribution of the rotor position angles, supported the validity of the proposed method.

1. Introduction

Permanent magnet synchronous machines (PMSMs) have a leading position nowadays in various fields of modern life due to their significant features. Compared to the relative machines, the PMSMs have a higher (power/size) ratio, greater reliability, lower power consumption, and faster speed. These features are the essential properties that make the PMSMs desirable in a wide range of industrial applications over other machines, starting from home appliances to complicated industrial processes [1]–[3].. The process of commutation is the fundamental factor in the best running of PMSMs. This process is strongly related to the prior knowledge of the position of the north pole of the rotor permanent magnet. So, accurate rotor position estimation is regarded as the crucial element to maintaining the optimum action of this type of machine. Based on this, various methods have been proposed to control this process on this type of motor at different speeds, from standstill to high speed. Among these methods, the proper start-up technique of PMSMs preserves reasonable posterior operation and avoids reverse running or stiffness of the rotor. Therefore, the prior accurate determination of the rotor position angle ensures a flexible and exact commutation for current excitations of the stator three windings of the undertaken motor. Accordingly, a soft motor running with minimum torque ripple and maximum output power can be taken out [4], [5].

The methods of rotor position valuation are categorized into three classes according to the region of machine speed; the standstill region, low-speed

* *Corresponding author.*
E-mail address: mazen.ali@qu.edu.iq (Mazen Al Ibraheemi)

https://doi.org/10.30772/qjes.v16i2.877

region, and medium/high speed. At medium and high speeds, many approaches have been proposed to estimate the rotor position. All of those approaches are based on the detected back-EMF. As this back-EMF is a function of motor speed, it becomes of a comparable value to the noise level at low rotor speed. This leads to an impaired signal-to-noise ratio (SNR) which hinders the employment of the back EMF in the algorithm of rotor position detection. Therefore, other methods have been presented to predict the rotor position angle at low speeds. The most popular one is based on the injection of a high-frequency signal in the stator windings. Then extraction of this high frequency through filters involves the required position information [9]. At zero speed, many efforts have been made, over the last two decades, to solve the problem of magnet polarity and rotor position because the back EMF disappears completely under this condition. A scheme was proposed in 1995 to estimate the position and speed of the rotor shaft of ac machine, including the start-up position, through injection of a 3-phase high-frequency signal and detecting the position by implementing a demodulation process to exploit the machine magnetic saliency track [10]. Reference [11] presented in 1997 an approach to determine the polarity of the non-salient pole and to estimate the position of the rotor dependent upon the saturation effect of stator iron core due to applying a pulse to the three stator windings and the resulting differences in the currents of the three phases. Another start-up technique for brushless dc motor (BLDCM) was presented in 2002 in which the stator was excited, and the period of discharge was employed to determine the rotor's initial position. To achieve that, the effect of magnetic saturation was used to show the difference in the discharge period, while a control system based on the Field Programmable Gate Array technique (FPGA) was added to interpret this time period and to define accordingly the rotor position with 60^0 resolution [12].

Another view for the start-up of BLDCM was also introduced in 2002 by [13], where it proposed the injection of six pulses in stator windings and testing the currents responses from which the standstill rotor position could be extracted by monitoring the stator inductances variations. Reference [14] suggested a novel view to sense the standstill rotor position of the Interior Permanent Magnet (IPM) motor relying on the considerable amount of magnetic flux linkage produced by the IPM. Correspondingly, this could cause a noticeable change in the inductances of rotor reference frame Ld and Lq which should involve information about zero-speed rotor position. Another detection method for IPM initial rotor position was introduced in [15] by injection of high-frequency carrier signals, whereas a second-order Taylor series for the relation between stator current and flux linkage in the d-axis rotor reference frame was used to detect the rotor polarity.

Reference [16] proposed, in 2003, a method for rotor position estimation by applying voltage pulses and measuring the peaks of resulting currents to achieve the goal. To avoid the uncertainty in values of current peaks, an iterative voltage sequence was combined with fuzzy logic processing of current responses. Reference [17] presented a 30^oresolution rotor position estimation by measuring the line-to-line back EMF when two windings are supplied with dc voltage. In 2006, [18] introduced a technique to detect the polarity of the magnet and the angle position of the rotor at zero speed. This initialization process was achieved by injecting a high-frequency signal and a sequence of current pulses composed of two pulses. Again, the saturation in the stator iron core was exploited here, moreover, the injected current should possess a value high enough to produce a noticeable change in iron saturation.

In the following year, 2007, [19] presented different views focusing on the design of machines to take into consideration the enhancement of machine ability to achieve accurate start-up. By this reference, a magnetic ring was added to form a bridge between the stator teeth. This modification increased the signal-to-noise ratio which contributed to improved detection for magnet polarity and angle position. Reference [20] investigated 2008 the robustness in the detection of the polarity and position of the permanent magnet rotor. In order to improve this robustness, two offsets were defined to be investigated and decoupled, they are; dc-offset vector and angular offset. In 2009, [21] proposed a method to expect a 30-degree resolution rotor position based on applying three voltage pulses and comparing the corresponding current responses which should be affected by the variation of the inductance due to the voltage pulses.

A modified design for a PMSM, type surface-mounted SPM, was proposed in [22] to be able to create self-magnetic saliency which allowed position estimation tracking. This was achieved through rotor zigzag leakage flux from surface permanent magnets. Reference [23] proposed in 2012 using three voltage pulses, in addition to the corresponding current responses, to achieve a rotor position estimation of 300 resolution in a brushless DC motor. The current responses were related to the changes in the stator inductances due to the saturation effect. It also was represented in 2015 with some improvements to overcome some requirements but the main trend was maintained [24].

This paper introduces a senseless approach to give an estimation of one-degree resolution to the position of the rotor at standstill for non-saturated PMSMs. It is based on sensing the terminal voltages and currents in two of the machine phases which come as responses to two short pulses applied to the stator coils to excite the machine at zero speed. As the given approach does not employ the magnetic saturation of stator iron, this makes it suitable for non-saturated, or weak-saturated, machines. The proposed method achieves an exact estimation for rotor position of 1^o resolution and does not require any technique for magnet polarity detection. Only two current sensors are required to achieve the estimation. The paper is organized into four sections. The first presents the introduction of this work. Section two explains the theoretical background. While sections three and four discuss the MATLAB proposed model and the conclusion respectively.

2. Theory

2.1 Voltages Measurements

In the 3-ph PMSM, two coils of the stator windings form a series combination that can be energized separately from the third winding, non-excited, which can be used to monitor the drops of voltages across those coils. Figure (1) illustrates applying a short pulse width, of 150 microseconds duration time, between the terminal of coil A and the terminal of coil B. The solid line shows the resultant current (Ion) which passes in their combination. Then, the voltage which is measured between the free side of the free coil, C, and the ground refers to the voltage drop between the terminal of coil B and the neutral point N. Therefore, this voltage is denoted as V_{NB1} where the subscribe '1' indicates the voltage measured during the first test pulse.

After 150μsec, the first test pulse elapses and the connection of the two excited coils, A and B, is reversed due to the absence of the exciting pulse which allows to flow of freewheeling current (I_{off}), shown by the dashed line. Accordingly, another voltage appears on the free terminal of coil C which indicates the drop voltage across coil A which is denoted by V_{NA1}.

The same events are repeated when the next pulse, the second, excites the two windings' series combination, coil A and coil C, while the third coil, B, is the free coil in this case, as illustrated by figure (2). Correspondingly, the voltages V_{NC2} and V_{NA2} emerge at the terminal of the free coil. The subscript '2' is to indicate the voltages that appeared when the 2nd pulse, of a duration of 150µsec, is applied.

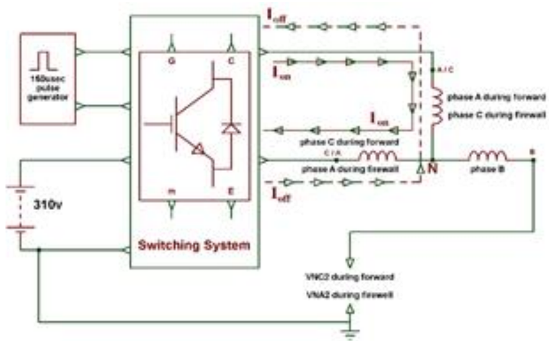

Figure 1. Coils A and B are energized by the first test pulse and the reaction of freewheeling.

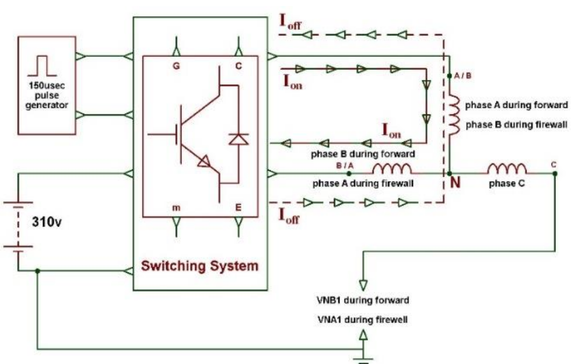

Figure 2. Coils A and C energizing by the second test pulse and the reaction of freewheeling

For instance, let's suppose the machine rotor is at the angle position 45°, then according to the proposed method, four voltages V_{NB1}, V_{NA1}, V_{NC2} and V_{NA2} are measured. These voltages are shown in figure (3). The figure has also shown the third drawing to four sampling pulses, each of 10µsec width and cantered at the positions 75, 225, 375, and 525µsec respectively. Another fourth drawing is also shown to illustrate the sampled values from the four measured voltages. The sampled values are to facilitate the comparisons among the voltages and, correspondingly, take the decision about the estimated position of the machine rotor.

The procedure of the voltage measurements and the angle position estimation was periodically repeated and applied for the machine rotor positions 0 through 360 degrees. The shapes of the corresponding four voltages, at the whole positions of the rotor, are drawn in figure (4). Each voltage shape can be divided into sectors as will be illustrated later. Four considerable comparisons correspond to the obtained values of the measured voltages: VNB1, VNA1, VNC2, and VNA2. The results of the comparisons can be exploited to distinguish different sectors within the whole space angles of the machine rotor. So, six sectors (each of width 30 degrees) in the rotor whole space can be created. The sectors are numbered from 1 to 6. These numbers will be used in the next section as an address line of memory. Table 1 summarises the coding of the voltage comparisons into six sectors.

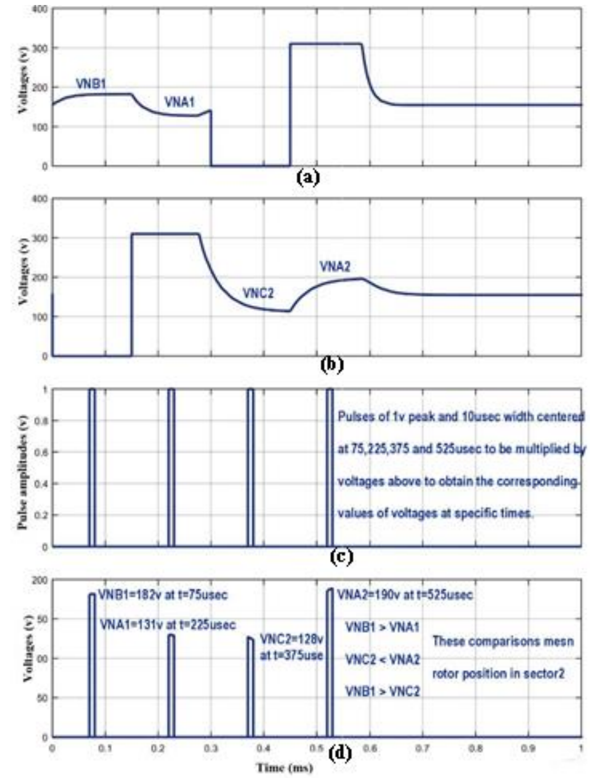

Figure 3. (a and b) Measured voltages when the machine rotor was at position 45 degrees, (c) Sampling pulses, (d) Sampled voltages.

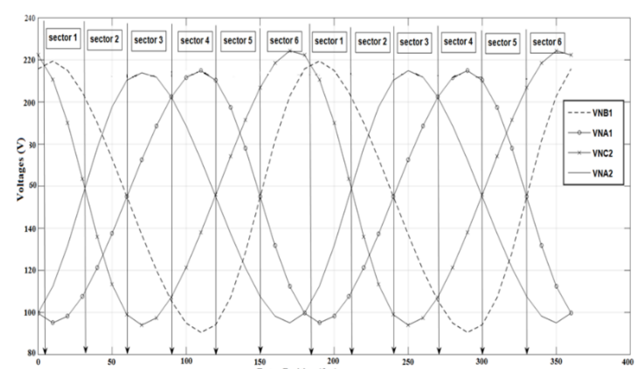

Figure 4. Measured voltages at the whole positions of the rotor.

Table 1. Voltage comparisons Coding to form the sectors and address line.

Voltage comparisons	Sectors Logical coding					
	1	2	3	4	5	6
$V_{NB1} > V_{NA1}$	1	1	0	0	0	1
$V_{NC2} > V_{NA2}$	1	0	0	0	1	1
$V_{NB1} > V_{NC2}$	1	1	1	0	0	0
$(x\text{-address})_2$	111	101	001	000	010	110
$(x\text{-address})_{10}$	7	5	1	0	2	6

The steps of extracting the x-address are illustrated in figure (5). Firstly, the machine voltage terminals are sensed, then compared and decoded and, eventually, the x-address is yielded.

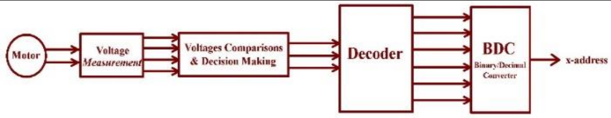

Figure 5. Measured voltages at the whole positions of the rotor.

2.2 Current Measurement

By each test pulse, a narrow duration forward and freewheeling successive currents are produced. These currents can be mathematically specified according to the following equations:

$$i(t) = \frac{V}{R}\left(1 - e^{-\frac{R}{L}t}\right) \quad (1)$$

$$i(t) = \frac{V}{R}\, e^{-\frac{R}{L}t} \quad (2)$$

where V is the peak voltage of the applied test pulse, R is the total resistance of the series combination of any two of the stator coils, and L is the total inductance of that series combination. Figure (6) shows two applied test pulses and the two currents, I_1 and I_2 that are produced by them. The drop voltage V_{NB1} can be written as:

$$\mathrm{V_{NB1}} = \mathrm{iR_B} + \mathrm{L_B}\frac{\mathrm{di}}{\mathrm{dt}} \quad (3)$$

From the current response, only the current portion of linear variation will be noticeable because the width of the test pulse is too short to view the full growth of the current. This case is highlighted in figure (6). Algebraically, this portion forms a straight line whose equation is given by the formula y=qx+k, where "q" represents the line slope and "k" is the intersection. Therefore, q= di/dt and a current can be deduced from eq(3) as the following:

$$\mathrm{i} = \frac{\mathrm{V_{NB1}} - \mathrm{qL_B}}{\mathrm{R_B}} \quad (4)$$

In this equation, only the voltage term is variable with the position of the machine rotor. Consequently, the duration of the current pulse is also related to the angle position of the rotor. For this purpose, the peak of the current response by the second test pulse was employed to predict the machine rotor position. Comparing the value of the time constant of the current growth in any two coils series combination with the duration of the test pulse shows that the pulse duration is just a small portion of the time constant. This feature allows testing the machine without causing any movement of the machine rotor.

The two test pulses as given by the MATLAB/Simulink are shown in Figure (6). Each pulse is of a total width of 300μsec and a 50% duty cycle. The shapes of the corresponding current responses are also illustrated. The chosen peak of the second current response is highlighted in the figure. This peak was employed in creating the second memory address, the y-address. The concept that stands behind y-address creation is highlighted in figure (7). Firstly, the peak value of the second current response, I_2, is sensed and measured. Then, the first common three digits in the current values are eliminated by the modification and amplification block. Meanwhile, the current response is also amplified and reformed by the residuals by this block. The deviation algorithm block is responsible for creating a considerable difference among the peaks of the current responses at different rotor angle positions. Nevertheless, some of the current residuals at the output of the algorithm block still have too close values to be distinguished. This problem does not allow the creation of a single determined y-address for each rotor angle value. To overcome this obstacle, specified numbers are stored in the shift memory block. The numbers are added to the residuals to make the required shift.

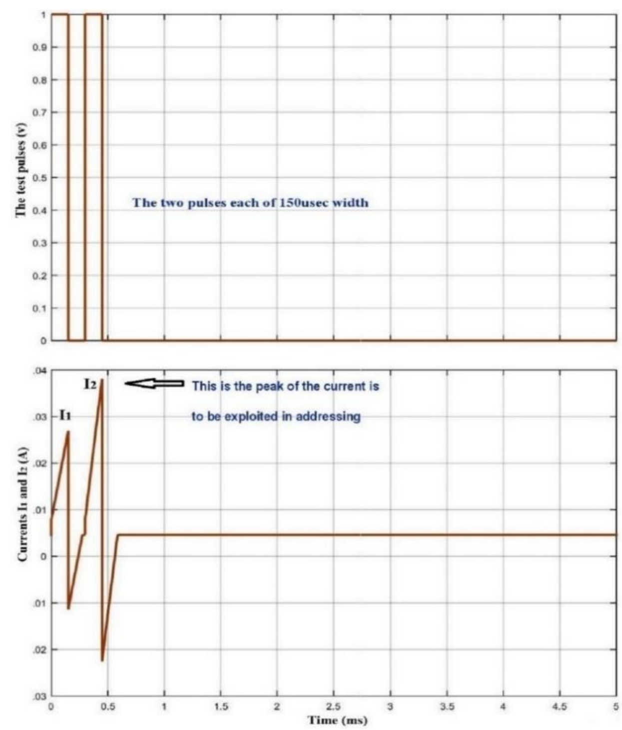

Figure 6. The two test pulses and the resultant current responses

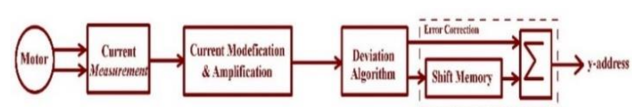

Figure 7. Steps in the creation of y-address

3. Results and Discussions

The mathematical model of this paper has been implemented, simulated and run by MATLAB/Simulink environment. Figure (8) shows the basic scheme of the simulated model. To meet the final goal of the paper, the exact angular positions of the rotor of PMSM under test have been stored in the cells of the memory block given in the model figure. The location of each cell is accessed through two address lines. The first line is denoted by the x-address which can be formed from the six sectors numbering within the rotor space. Thereby, the memory size is divided into six divisions, each determining the rotor's proper position within the specified sector. The second line is labeled by the y-address line. The value of this address is specified by the peak of the measured current. The intersection of the x and y lines permits to access the required memory cell where the value of the rotor angle is stored.

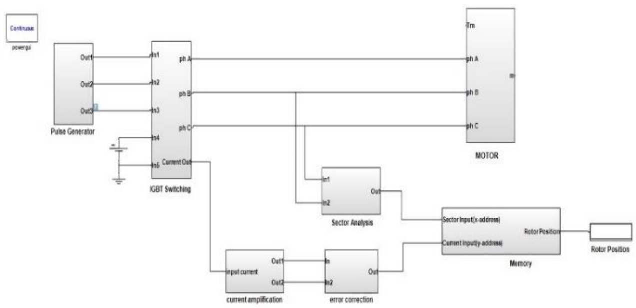

Figure 8. The proposed method implemented.

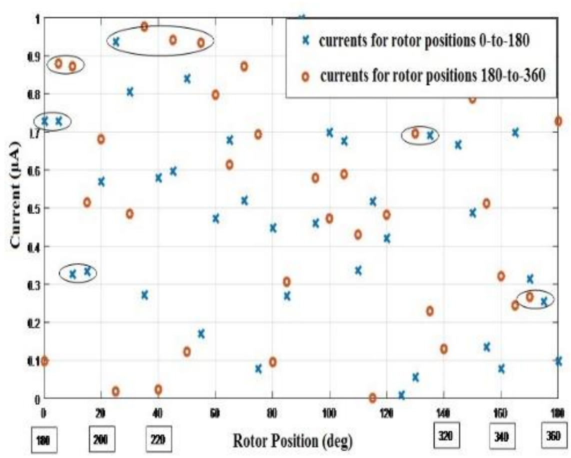

Figure 9. Values of current peaks over the whole angular spatial of the rotor

Table 2. Parameters of the machine under test

Item	Property
Number of phases	3
Type of rotor	Salient
Stator Phase Resistance	2 Ohms
Stator Inductance	L_q = 1.25H , L_d = 0.75H
Flux Linkage	0.285757 (V.s)
Inertia,	0.621417(g.m^2) ,
Viscous amping	0.303448(mN.m.s)
DC Link Voltage	310V

Specifications of the machine under simulation are illustrated in table 2. Figure (9) shows 360 values of the current peaks for the angles of the machine rotor positions from 0^o to 36o^o which were measured by the proposed model. The symbols 'x' and 'o' indicate the current peak values of the angle positions from $\mathbf{0^o}$ to $\mathbf{180^o}$ and from $\mathbf{180^o}$ to $\mathbf{360^o}$ respectively. It appears from this figure that the model has succeeded in exploiting the machine magnetic anisotropic properties to locate a certain peak current value for each rotor position, within the specified sector, even for the $\mathbf{180^o}$ reversed positions which made it possible to pass the need for searching rotor magnet polarity. The obtained values for current peaks were very close to each other which made it not possible to be employed in addressing the memory, so a certain algorithm based on exponential function was used to make significant differences between those peak values and to achieve the results presented in figure (9).

4. Conclusion

The proposed simulated model presents an accurate rotor position expectation of 1^o resolution with a 1% error for non-saturated permanent machines. Accordingly, it is reliable to take the output of memory directly to the commutation process controller to start running the machine. The model has successfully produced the same estimation accuracy when tested for both one-pair and two-pairs PMSM and it could be used with any other pole-pairs number. Although the work was applied on a salient machine, it can be modified to be applicable to the non-salient, round, PMSM. The proposed algorithm to exploit and amplify the microampere differences in current response contributes widely to substituting the technique of magnet polarity test. However, two currents I1 and I2 are the resultants from the utilization of the two test pulses, but, only one of them is required to achieve the process of y-address extraction, I2 was chosen in this work.

Authors' contribution

All authors contributed equally to the preparation of this article.

Declaration of competing interest

The authors declare no conflicts of interest.

Funding source

This study didn't receive any specific funds.

REFERENCES

[1] M. M. A. Al Ibraheemi, z. H. Radhy, f. J. Anayi, and H. Al Ibraheemi, "Memorized Approach for Implementation of Space Vector Pulse Width Modulation," *period. Eng. Nat. Sci.*, vol. 7, no. 4, pp. 1892–1903, 2019.

[2] M. S. Mubarok, t. H. Liu, c. Y. Tsai, and Z. Y. Wei, "A Wide-Adjustable Sensorless Ipmsm Speed Drive Based on Current Deviation Detection Under Space-Vector Modulation," *energies*, vol. 13, no. 17, 2020.

[3] M. Siami, d. A. Khaburi, m. Rivera, and J. Rodríguez, "A Computationally Efficient Lookup Table Based Fcs-Mpc for Pmsm Drives Fed by Matrix Converters," *Ieee trans. Ind. Electron.*, vol. 64, no. 10, pp. 7645–7654, 2017.

[4] J. Pando-acedo, e. Romero-cadaval, m. I. Milanes-montero, and F. Barrero-gonzalez, "Improvements on A Sensorless Scheme for A Surface-Mounted Permanent Magnet Synchronous Motor Using Very Low Voltage Injection," *Energies*, Vol. 13, no. 11, 2020.

[5] Reigosa, D. D., Fernandez, D., Zhu, Z. Q., et al.: 'Pmsm Magnetization State Estimation Based on Stator-Reflected Pm Resistance Using High-Frequency Signal Injection', Ieee Trans. Ind. App., vol. 51, no. 5, pp. 3800-3810, Sept./oct. 2015.

[6] Jash, K., Saha, P. K., Panda, G. K.: 'Vector Control of Permanent Magnet Synchronous Motor Based on Sinusoidal Pulse Width Modulated Inverter with Proportional Integral Controller', Int. Journal of Engineering Research and Applications, Vol. 3, No. 5, Pp. 913-917, Sept./Oct. 2013.

[7] Li, Y., Zhu, Z. Q., Howe, D., Et Al.: 'Improved Rotor-Position Estimation by Signal Injection in Brushless Ac Motors, Accounting for Cross-Coupling Magnetic Saturation', Ieee Trans. Ind. Appl., Vol. 45, No. 5, Pp. 1843-1850, Sept./Oct. 2009.

[8] Patric, L. J., Robert, D. L.: 'Transducerless Position and Velocitv Estimation in Induction and Salient Ac Machines', Ieee Trans. Ind. App., Vol. 31, No. 2, Pp. 240-247, Mar./Apr. 1995.

[9] Peter, B. S., Gasperi, M. L., Ray, G., Et Al.: 'Initial Rotor Angle Detection

of a Non-Salient Pole Permanent Magnet Synchronous Machine', Ieee Ind. App. Society Annual Meeting, New Orleans, Louisiana, October 5-9, 1997.

[10] Lai, Y. S., Shyu, F. S. Tseng, S. S.: 'New Initial Position Detection Technique for Three-Phase Brushless Dc Motor Without Position and Current Sensors', Ieee Ind. App. Conference, 37th Ias Annual Meeting, Pittsburgh (Usa), Oct. 2002.

[11] Jang, G. H., Park, J. H., Chang, J. H.: 'Position Detection and Start-Up Algorithm of a Rotor In A Sensorless Bldc Motor Utilising Inductance Variation', Iee Proceedings -Electric Power Appl, Vol. 149, No. 2, Pp. 137-142, Mar. 2002.

[12] Kim, H., Huh K. K., Lorenz, R. D. Et Al.: 'A Novel Method for Initial Rotor Position Estimation for Ipm Synchronous Machine Drives', Ieee Ind. App., Vol. 2, Pp. 1173-1180, Oct. 2003.

[13] Jeong, Y., Lorem, R. D., Jahns, T. M., Et Al.: 'Initial Rotor Position Estimation of An Interior Permanent Magnet Synchronous Machine Using Carrier-Frequency Injection Methods', Ieee Inte. Elec. Machines, Vol. 2, Pp. 1218-1223, Jun. 2003.

[14] Tursini, M., Petrella, R., Parasiliti, F.: 'Initial Rotor Position Estimation Method for Pm Motors', Ieee Trans. Ind. App., Vol. 39, No. 6, Pp. 1630-1640, Dec. 2003.

[15] Medjmadj, S., Diallo, D., Mostefai, M., Et Al.: 'Pmsm Drive Position Estimation: Contribution to The High-Frequency Injection Voltage Selection Issue', Ieee Trans. Energy Conversion, Vol. 30, No. 1, Pp. 349-358, Mar. 2015

[16] Holtz, J.: 'Initial Rotor Polarity Detection and Sensorless Control of Pm Synchronous Machines', Ieee Ind. App. Conference, 41st Annual Meeting, Tampa (Fl), Vol. 4, Pp. 2040-2047, Oct. 2006.

[17] Akatsu, K., Harke, M. C., Lorenz, R. D.: 'Spmsm Design Considerations for Initial Position and Magnet Polarity Estimation Using Carrier Signal Injection', Ieee Ind. App. Conference, 42nd Annual Meeting, New Orleans (La), PP. 2393-2398, Sept. 2007.

[18] Raca, D., Harke, M. C., Lorenz, R. D.: 'Robust Magnet Polarity Estimation for Initialization of Pm Synchronous Machines with Near-Zero Saliency', Ieee Trans. Ind. App., Vol. 44, No. 4, Pp. 1199-1209, Aug. 2008.

[19] P. Champa, P., Somsiri, P., Wipasuramonton, P., Et Al.: 'Initial Rotor Position Estimation for Sensorless Brushless Dc Drives', Ieee Trans. Ind. App., Vol. 45, No. 4, Pp. 1318-1324, Aug. 2009.

[20] Yang, S. C., Suzuki, T., Lorenz, R. D., Et Al.: 'Surface Permanent Magnet Synchronous Machine Design for Saliency-Tracking Self Sensing Position Estimation at Zero and Low Speeds', Ieee Energy Conversion Congress Exposition, Pp. 3493-3500, Sept. 2010.

[21] Pillai, N. S., Salitha, K., Abraham, C.: 'Analysis and Simulation Studies for The Estimation of Rotor Position in Sensorless Bldc', International Journal Of Electrical And Electronics Engineering (Ijeee), Vol. 2, No. 1, Pp. 86-90, 2012.

[22] Pillai, N. S., Vipin, A. M., Radhakrishnan, R.: 'Analysis and Simulation Studies for Position Sensorless Bldc Motor Drive with Initial Rotor Position Estimation', Ieee, Inter. Conf. On Nascent Technologies in The Engineering Field, Navi Mumbai, Jan. 2015.